

Innovative Approaches to Scour Mitigation: A Study on Modified Bridge Piers and Collars

S.T.Vijaya Sarada¹ & Gummadi Venkata Rao²

¹Research Scholar, Department of Civil Engineering, Anurag University, Hyderabad

²Professor, Department of Civil Engineering, Anurag University, Hyderabad

Abstract

Bridge scour, the removal of sediment from around bridge piers due to flowing water, is a critical factor contributing to bridge failures worldwide. Effective countermeasures are essential to ensure the safety and longevity of bridge structures. This study investigates the influence of pier geometry and collar arrangements on the reduction of local scour under clear-water conditions. Laboratory experiments were conducted in a glass-walled mobile bed flume using four pier shapes: circular, elliptical, parabolic, and lenticular. Each pier was tested both with and without collars installed at four configurations: at the bed level (BL), one pier diameter below the bed level (1DBBL), one diameter above (1DABL), and a double collar setup (DC). The experiments were performed at two flow depths (12 cm and 14 cm) and monitored for seven hours each to capture the temporal variation of scour depth. Results revealed that the lenticular pier consistently achieved the highest scour reduction across all configurations, especially when combined with the double collar arrangement. For example, at a 12 cm flow depth, the lenticular pier with a double collar reduced scour by up to 82.60% compared to a circular pier without a collar. Tandem arrangements of piers further demonstrated the influence of pier positioning on scour behavior, with downstream piers generally benefiting from reduced scour due to sheltering effects. The findings underscore the effectiveness of combining geometric modifications with strategic collar placement in mitigating local scour, offering practical insights for bridge design and maintenance.

Keywords: Local scour; bridge pier; collar; scour reduction; pier shape; hydraulic experiment.

1. Introduction

Scour around bridge piers and abutments is a critical hydraulic phenomenon and one of the foremost causes of bridge failures worldwide. It involves the removal of sediment from the foundation region due to high-velocity flows, which lead to the formation of scour holes, undermining structural stability. The United States Federal Highway Administration (FHWA) attributes over 60% of documented bridge collapses to scour-related mechanisms. In India, several notable failures, including the Maddur Railway Bridge, Kadalundi Bridge, and the Savitri River Bridge, have been associated with scour during high-flow events, emphasizing the urgency of implementing effective scour mitigation strategies.

The local scour process is driven primarily by complex interactions between the flow field and the bridge pier geometry. At the upstream face of a pier, the deceleration of flow results in increased pressure and downward flow, initiating the development of horseshoe vortices. These vortices, in combination with wake vortices at the downstream side, generate localized erosion that deepens and widens with time. Figure 1 illustrates the flow pattern around a typical bridge pier, highlighting the influence of downflow and vortex formation on sediment removal. While advancements in structural design have enhanced bridge resilience, local scour remains a persistent and dynamic

challenge, particularly under clear-water conditions where sediment transport is minimal but erosion potential is high. Several countermeasures have been developed to reduce scour, including riprap, geobags, concrete mats, and flow-altering devices. Among these, collars have shown considerable promise due to their simplicity, cost-effectiveness, and hydraulic efficiency. By acting as flow deflectors, collars reduce the strength of downflow and associated vortex systems, thus protecting the bed material from erosion. The efficiency of collars is significantly influenced by their geometry, installation depth, and integration with the pier shape.

Pier geometry itself plays a vital role in influencing the flow structure and subsequent scour formation. Conventional cylindrical piers present a broad upstream face to the flow, exacerbating vortex formation and sediment removal. Conversely, streamlined and modified shapes such as elliptical, parabolic, and lenticular profiles can reduce the effective flow obstruction, thereby mitigating vortex strength and limiting scour development. Despite extensive studies on either collars or pier shapes independently, there exists limited research on their combined effects, especially in the context of group pier arrangements where flow-pier interactions become more complex. This study addresses this gap through a comprehensive experimental investigation of scour around isolated and tandem arrangements of circular and modified piers, both with and without collars. The aim of this study is to evaluate how pier shape and collar positioning interact to influence scour characteristics, and to identify configurations that offer optimal protection against local scour. The findings of this study have the potential to inform practical bridge design and maintenance strategies, especially in regions prone to extreme hydraulic events.

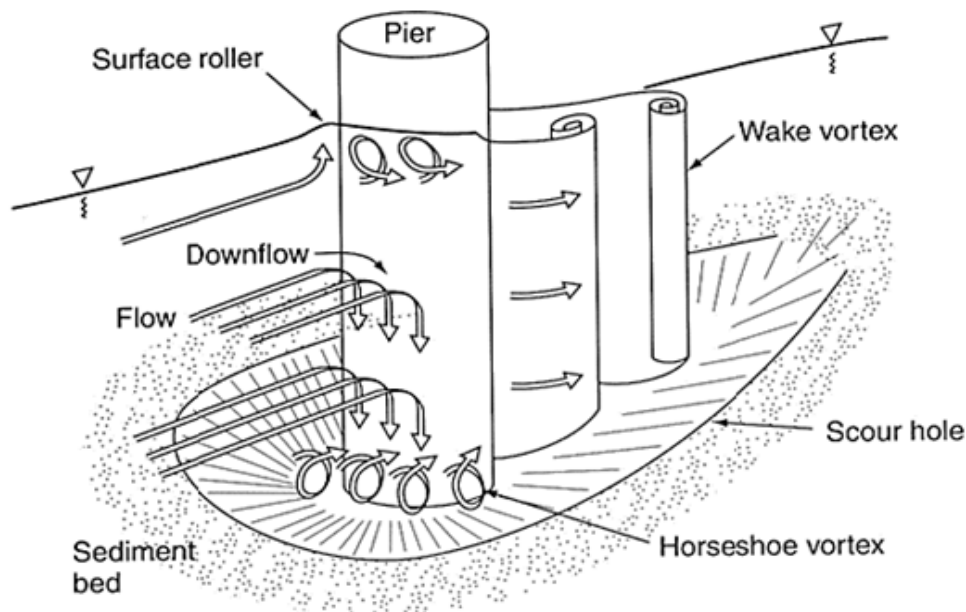


Figure 1. Flow pattern around bridge piers (source: Kothyari, 2007).

2. Literature Review

Scour around bridge piers is a well-documented cause of structural instability, and numerous studies have highlighted its role in bridge failures worldwide. Melville and Coleman (2000) identified scour as a major contributor to bridge collapse, attributing it to the interaction between hydrodynamic forces and sediment transport. Shen et al. (1969) categorized scour into two main types: clear-water scour, which occurs in the absence of sediment transport, and live-bed scour, which involves continuous sediment movement. Chiew and Melville (1987) emphasized that scour depth depends on flow intensity, pier geometry, sediment characteristics, and hydraulic conditions. To counteract these effects, researchers have proposed various structural measures such as riprap, geobags, slots, and collars. While effective to varying degrees, the performance of these countermeasures depends on site-specific factors including flow conditions and bed material (Kothyari, 2007). Among these, collars have gained prominence due to their cost-effectiveness and ability to disrupt downflow and horseshoe vortex systems that drive scour (Melville and Hadfield, 1999).

2.1 Influence of Pier Geometry on Scour Reduction

Pier geometry plays a critical role in controlling local scour. Breusers et al. (1977) demonstrated that the effective width of a pier's upstream face directly influences scour depth—wider piers lead to more extensive scour. Grimaldi et al. (2009) and Mubeen Beg et al. (2013) showed that streamlined pier shapes can reduce the intensity of downflow and associated vortices, thereby mitigating sediment erosion. Several modified pier geometries have been studied. Elliptical piers, due to their elongated form, delay flow separation and reduce vortex strength (Zarrati et al., 2004). Parabolic piers offer a gradual transition in shape that minimizes abrupt pressure changes, leading to reduced scour (Tseng et al., 2000). Lenticular piers, characterized by a tapered cross-section, reduce the effective width at the upstream face, thereby minimizing flow disturbance and associated scour (Alireza et al., 2017). Despite these advantages, limited research has been conducted on the combined effects of pier geometry and collar arrangements, which presents an important opportunity for further study.

2.2 Effectiveness of Collars as a Scour Countermeasure

Collars act as flow-altering devices that weaken the downflow and horseshoe vortices responsible for scouring. Moncada et al. (2009) found that collars installed at bed level significantly reduce scour compared to piers without collars. Heidarpour et al. (2010) showed that a double-collar arrangement (one at bed level and another at an elevated position) can provide greater protection by mitigating sediment removal across multiple depths. Further research by Zarrati et al. (2004) and Mashahir et al. (2006) confirmed that collar performance is sensitive to placement and size. Collars installed at the bed level are most effective, while those below bed level allow scour holes to form above them, diminishing their utility. Mohammad et al. (2010) noted that collar diameter is also a determining factor, with sizes 2–3 times larger than the pier diameter offering optimal protection. These studies underscore the potential of collars as a simple yet powerful countermeasure when properly designed and positioned.

2.3 Research Gaps and Study Justification

While numerous studies affirm the individual benefits of modified pier shapes and collar applications, relatively few have investigated their combined impact. Existing research tends to focus either on optimizing pier geometry (e.g., Kothiyari et al., 1992) or evaluating collar positioning (Melville et al., 2008), but not both in an integrated experimental framework. The present study aims to address this gap by conducting controlled flume experiments to evaluate the performance of elliptical, parabolic, and lenticular piers, each combined with different collar placements, including at the bed level, above, below, and in a double-collar configuration. A comparison is also made against conventional circular piers under identical hydraulic conditions. By systematically examining these variables, this study contributes to the development of integrated, cost-effective, and resilient design strategies for scour reduction around bridge piers.

3. Experimental Methodology

This experimental study was conducted to systematically investigate the influence of bridge pier geometry and collar placement on local scour under controlled clear-water flow conditions. A series of 62 laboratory experiments were designed and executed using a glass-walled mobile bed flume. The study includes both isolated and tandem pier arrangements, with four pier shapes tested across five collar configurations and two flow depths. The goal was to quantify scour depth variations and identify optimal configurations that minimize local scour.

3.1 Experimental Setup

The experiments were conducted in a 7.6-meter-long, 0.5-meter-wide, and 0.56-meter-deep glass-walled flume, located in the hydraulics laboratory. A 5.6-meter-long test section was provided centrally along the flume to ensure fully developed flow conditions before the pier model. To simulate the riverbed, a non-cohesive sediment layer with a median particle diameter $d_{50} = 0.28$ mm and geometric standard deviation $\sigma_g = 1.66$ was used. Figure 2 shows the actual flume setup, while a schematic diagram is provided in Figure 3.



Figure 2. Image of experimental setup.

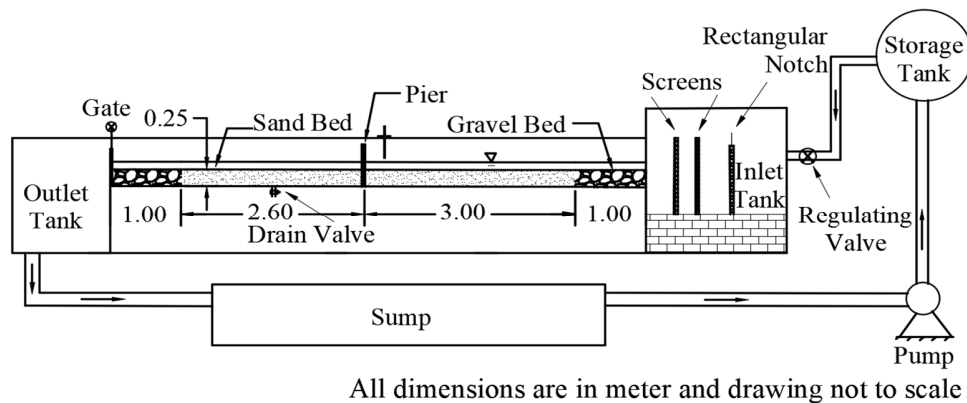


Figure 3. Schematic diagram of experimental setup.

A gravel transition section of 1 meter was placed at both upstream and downstream ends of the test section to stabilize the flow and avoid bed material washout. Flow was recirculated using a 40 HP centrifugal pump, and the flow rate was measured accurately using a calibrated rectangular notch with a 0.7-meter crest length. Two flow depths were selected: 12 cm and 14 cm. These depths correspond to clear-water flow velocities of 0.136 m/s and 0.165 m/s, respectively. The critical velocity V_c was calculated to be 0.26 m/s using Equation 1. This yielded velocity ratios V/V_c of 0.523 and 0.635, confirming the clear-water condition. Table 1 lists all the hydraulic parameters used for the experiments, including Froude and Reynolds numbers. Scour depth and water surface elevation were measured using a high-precision digital point gauge with an accuracy of 0.1 mm. Before each experiment, the bed was uniformly leveled using a scraper, and the pier model was installed vertically at the centerline, 4 meters downstream from the inlet.

$$V_c = 1.41[(S_s - S) \times g \times d_{50}]^{0.5} \left(\frac{Y}{d_{50}}\right)^{1/6} \quad (1)$$

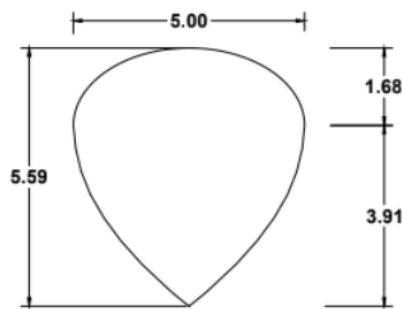
Where, S_s is the specific gravity of water (taken as 1.0), g is the acceleration due to gravity (9.81 m/s²), d_{50} is the median diameter of bed material particles (m), and Y is the flow depth (m).

Table 1: List of parameters considered to perform experiments

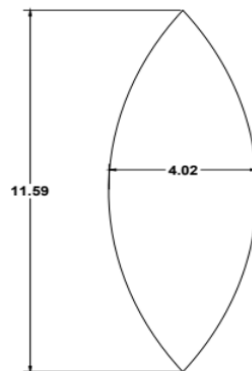
S. No.	Parameter	Value
1	Pier width (D) Shen et al. (1996)	5cm
2	Particle size (d_{50})	0.28mm
3	Geometric standard deviation (σ_g)	1.66
4	Flow depth (Y)	12cm & 14cm
5	Critical velocity (V_c)	0.26m/s
6	Flow velocity (V)	0.136m/s & 0.165m/s
7	Velocity ratio (V/V_c)	0.523 & 0.635 (<1)
8	Discharge (Q)	8.16 l/s & 11.63 l/s
9	Froude number (Fr)	0.1253 & 0.1407
10	Reynolds number (Re)	16320 & 19800

3.2 Pier Models and Collar Configurations

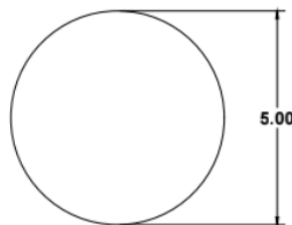
Four different pier shapes were tested in the study: circular, elliptical, parabolic, and lenticular. All pier models were made of polished teak wood and had equal cross-sectional areas to ensure shape-based comparisons were isolated from area-related effects. A schematic representation of the pier shapes is provided in Figure 4. The circular pier served as a control, while the three modified shapes were selected based on their potential to reduce effective width at the upstream face and minimize vortex formation.



(a) Stream line shaped pier



(b) Lenticular pier



(c) Circular pier

Figure 4. Schematic diagram of pier models (a) stream line pier, (b) lenticular pier, and (c) circular pier

To study the effect of collar placement, rectangular collars with a width of 14 cm were fabricated and installed around each pier. The following five configurations were tested for each pier shape:

- 1. Without collar
- 2. Collar at bed level (BL)
- 3. Collar at 1D below the bed level (1DBBL)
- 4. Collar at 1D above the bed level (1DABL)
- 5. Double collar (DC): One at BL and one at 1DABL

The dimensionless scour depth ratio h_s/D was used for comparative analysis across shapes and conditions.

3.3 Experimental Procedure

Each experiment was conducted for a continuous duration of seven hours to ensure that equilibrium scour depth was reached. The flow was introduced gradually using a regulating valve to prevent the initial displacement of sediment. After establishing the target flow depth and velocity, measurements of water level and scour depth were taken at fixed time intervals. The same procedure was repeated for each pier shape under all five collar conditions and both flow depths. The development of the scour hole was monitored both temporally and spatially, and its final depth was used as the basis for analysis. Observations were made visually and through the point gauge, with particular attention paid to the scour pattern around the upstream face where horseshoe vortices are most intense. The number and types of experiments on isolated piers are summarized in Table 2, which includes 40 experiments (4 pier shapes \times 5 collar configurations \times 2 flow depths).

Table 2: Experiments performed for a single pier with and without collar

Y (cm)	Condition	Circular	Ellipse	Parabola	Lenticular
12, 14	Without collar	2	2	2	2
	Collar at bed level	2	2	2	2
	Collar at 1D below bed level	2	2	2	2
	Collar at 1D above bed level	2	2	2	2
	Double collar (one at bed level and one at above 1D bed level)	2	2	2	2

3.4 Tandem Pier Arrangements

To examine the effect of pier interactions on scour, additional tests were performed with two and three piers arranged in tandem. The center-to-center spacing between piers was maintained at $S/D = 3$, where S is the spacing and D is the pier diameter (5 cm). These arrangements allowed for the evaluation of both reinforcing effects (on the front pier) and sheltering effects (on the rear pier).

Ten configurations of two piers in tandem were tested, including combinations such as CET (Circular–Elliptical Tandem), LCT (Lenticular–Circular), and PCT (Parabola–Circular). These are detailed in Table 3. Twelve configurations of three piers in tandem were also tested. Some examples include LECT (Lenticular–Elliptical–Circular Tandem) and CPLT (Circular–Parabola–Lenticular Tandem). All such combinations are listed in Table 4. Scour depth was recorded individually around each pier within the tandem setups, allowing comparative evaluation across pier positions (front, middle, rear).

Table 3: Different arrangement of two piers in tandem






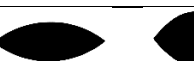























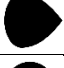








Notation	Arrangement
<i>CET</i>	
<i>CPT</i>	
<i>CLT</i>	
<i>LCT</i>	
<i>LET</i>	
<i>LPT</i>	
<i>ECT</i>	
<i>ELT</i>	
<i>PCT</i>	
<i>PLT</i>	

Table 4: Different arrangement of three piers in tandem

Notation	Arrangement
<i>LECT</i>	
<i>LCPT</i>	
<i>LCET</i>	
<i>LPCT</i>	

<i>CELT</i>			
<i>CLPT</i>			
<i>PCLT</i>			
<i>PLCT</i>			
<i>ELCT</i>			
<i>ECLT</i>			
<i>CLET</i>			
<i>CPLT</i>			

4. Results and Discussion

This section presents the results obtained from experiments with isolated piers with and without collars of different flow depths. Subsequently, the results obtained from experiments conducted on piers placed in tandem arrangements (two and three piers in a line) are presented and discussed.

4.1 Scour development around circular pier

The circular pier, used as the baseline model, exhibited the highest maximum scour depths under both tested flow conditions. For flow depths of 12 cm and 14 cm, the maximum scour depth ratios (h_s/D) were found to be 1.38 and 1.66, respectively. These results align with predictions from empirical models, as listed in Table 5. The temporal variation of scour, shown in Figures 5 and 6, indicates that scour depth increases rapidly in the initial hours and gradually stabilizes over time, confirming clear-water conditions with localized sediment entrainment.

Table 5: Comparison of circular pier observations without collar in $Y = 12$ cm and 14 cm

Sl. No.	Study	$Y = 12$ cm	$Y = 14$ cm
1	Present study	1.38	1.66
2	Laursen and Toch (1956)	1.755	1.838
3	Shen et al. (1969)	1.05	1.184
4	IRC (2000)	1.76	2.23
5	Lacey	1.72	1.6
6	HEC 18	1.22	1.36

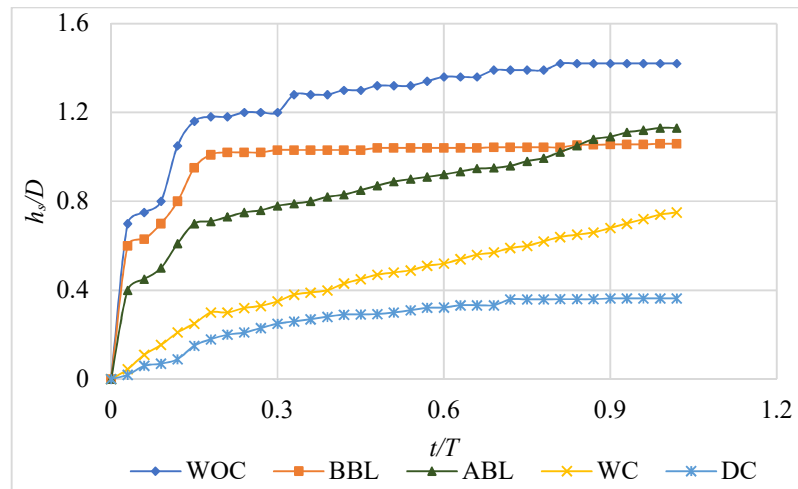


Figure 5: Temporal variation of scour depth ratio around circular pier for various conditions at 12 cm flow depth

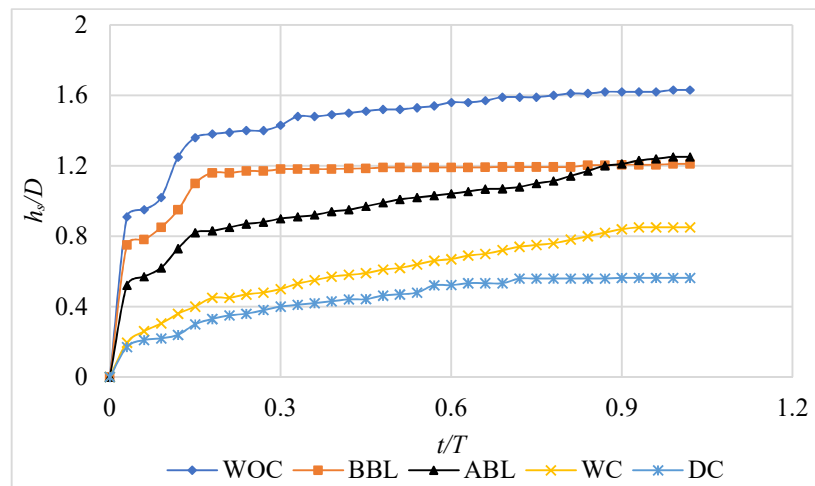


Figure 6: Temporal variation of scour depth ratio around circular pier for various conditions at 14 cm flow depth

When collars were introduced, scour depth reductions varied based on collar placement, as summarized in Table 6 and Table 7. The reduction percentages compared to the circular pier without a collar are as follows:

- Bed Level (BL): Reduction of 47.82% for $Y = 12$ cm and 42.16% for $Y = 14$ cm.
- 1D Below Bed Level (1DBBL): Reduction of 21.73% ($Y = 12$ cm) and 24.09% ($Y = 14$ cm).
- 1D Above Bed Level (1DABL): Reduction of 15.94% ($Y = 12$ cm) and 20.48% ($Y = 14$ cm).
- Double Collar (DC, BL + 1DABL): Reduction of 72.46% ($Y = 12$ cm) and 65.06% ($Y = 14$ cm).

Table 6: Scour depth ratios around different shaped piers with 12 cm flow depth

Y (cm)	Condition	h_s/D			
		Circular	Ellipse	Parabola	Lenticular
12	Without collar	1.38	1.34	1.32	1.15
	Collar at bed level	0.72	0.68	0.6	0.34
	Collar at 1D below bed level	1.08	1.02	1	0.92
	Collar at 1D above bed level	1.16	1.1	1	0.48
	Double collar (one at bed level and one at 1D above bed level)	0.38	0.34	0.3	0.2

Table 7: Scour depth ratios around different shaped piers with 14 cm flow depth

Y (cm)	Condition	h_s/d			
		Circular	Ellipse	Parabola	Lenticular
14	Without collar	1.66	1.6	1.54	1.425
	Collar at bed level	0.96	0.9	0.82	0.62
	Collar at 1D below bed level	1.26	1.2	1.12	1
	Collar at 1D above bed level	1.32	1.22	1.14	0.78
	Double collar (one at bed level and one at 1D above bed level)	0.58	0.54	0.42	0.32

Three experiments were conducted for a circular pier at a flow depth of 14 cm under identical conditions to ensure result reliability. The maximum scour depth values showed a variation of only 2%, indicating high repeatability. Temporal scour development trends from all three runs were consistent, with minor fluctuations, as illustrated in Figure 7. This confirms the robustness of the experimental setup and the reliability of the observed scour behavior for circular piers. Figures 8 and 9 compare the present study with Mia and Nago (2003) and Zarrati et al. (2004) for circular piers without and with collars, respectively. The maximum scour depths are in close agreement: 1.38D vs. 1.41D (without collar) and 0.96D vs. 0.98D (with collar at bed level). While minor variations exist in temporal development, the overall trends are similar, validating the present results and supporting further experiments on other pier shapes.

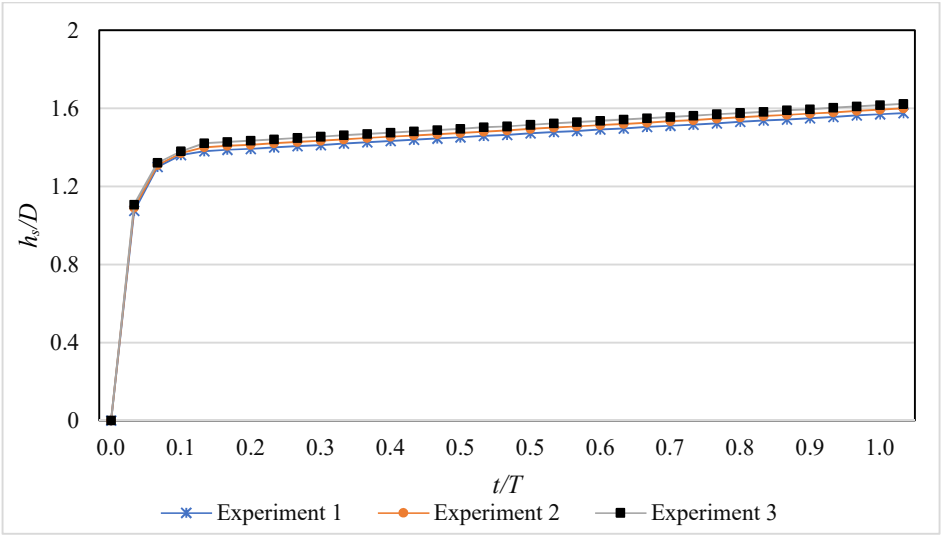


Figure 7: Temporal variation of local scour depth ratio for identical experiments

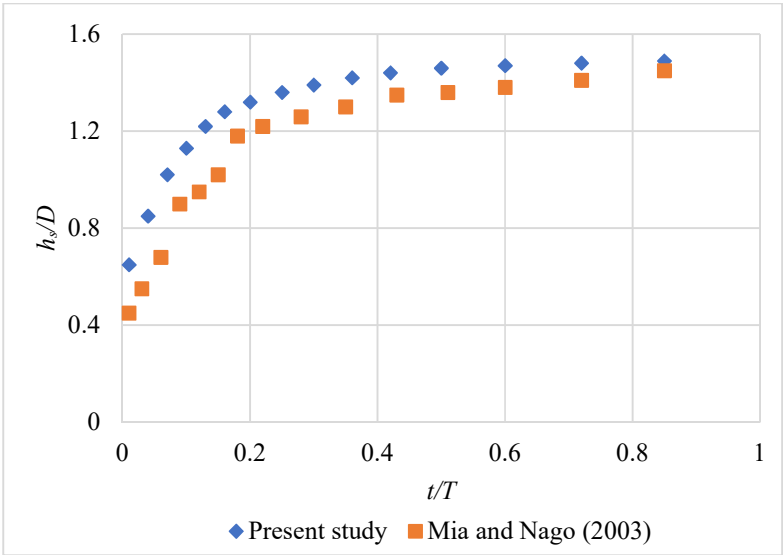


Figure 8: Comparison of present study with Mia and Nago (2003) in case of scour depth ratio around circular pier without collar

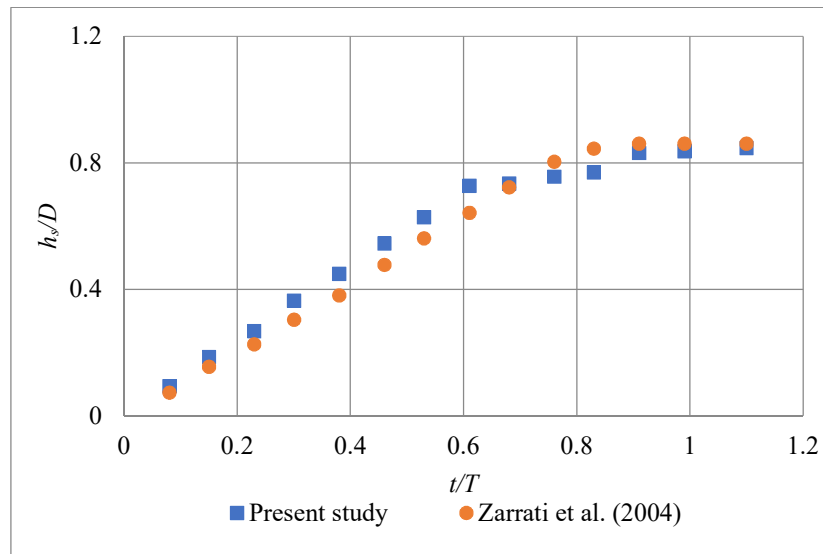


Figure 9: Comparison of present study with Zarrati et al. (2004) for circular pier with collar at bed level.

4.2 Scour Reduction in Modified Pier Shapes

To assess the impact of pier geometry, scour depths around elliptical, parabolic, and lenticular piers were compared against the circular pier under similar flow conditions. The following maximum scour depths were observed for piers without collars, as recorded in Table 6 and Table 7:

- Elliptical Pier: 1.34D (Y = 12 cm), 1.6D (Y = 14 cm)
- Parabolic Pier: 1.32D (Y = 12 cm), 1.54D (Y = 14 cm)
- Lenticular Pier: 1.15D (Y = 12 cm), 1.425D (Y = 14 cm)

These results indicate that modified pier shapes reduce scour depth compared to circular piers, with lenticular piers providing the most significant reduction. Figure 10 and Figure 11 show the temporal scour development for the elliptical pier, while Figure 12 and Figure 13 present similar trends for the parabolic pier. Figure 14 and Figure 15 illustrate that lenticular piers consistently experience the lowest scour depths, reinforcing their superior hydraulic performance.

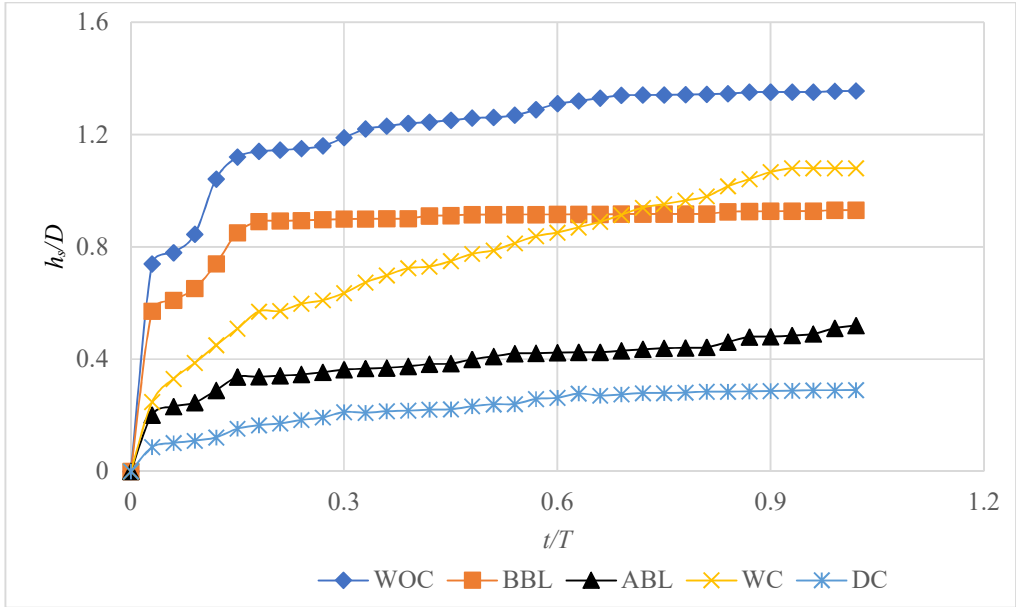


Figure 10: Temporal variation of scour depth ratio around Ellipse faced pier for various conditions at 12 cm flow depth

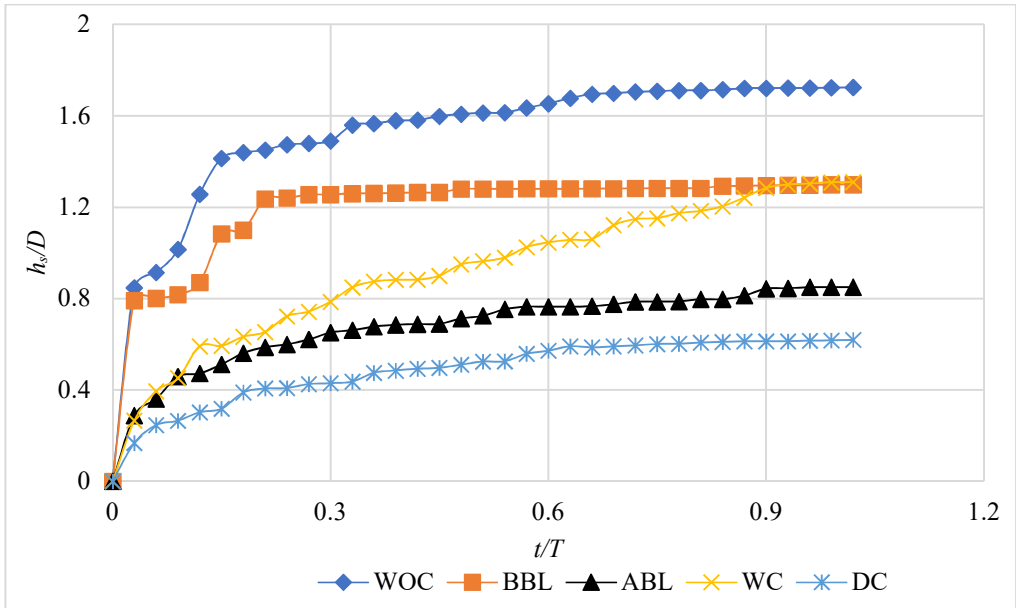


Figure 11: Temporal variation of scour depth ratio around Ellipse faced pier for various conditions at 14 cm flow depth

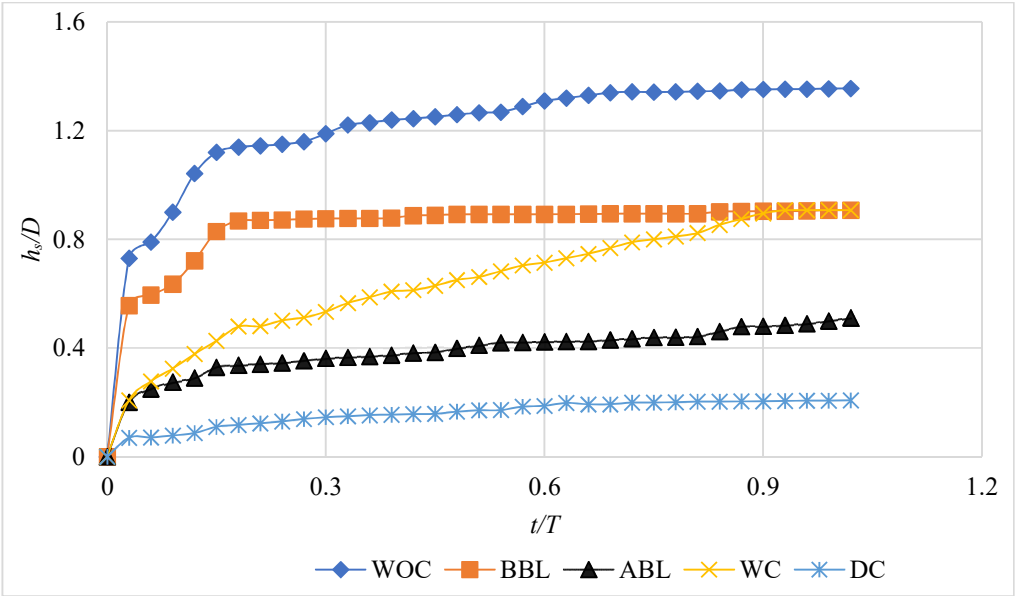


Figure 12: Temporal variation of scour depth ratio around Parabola faced pier for various conditions at 12 cm flow depth

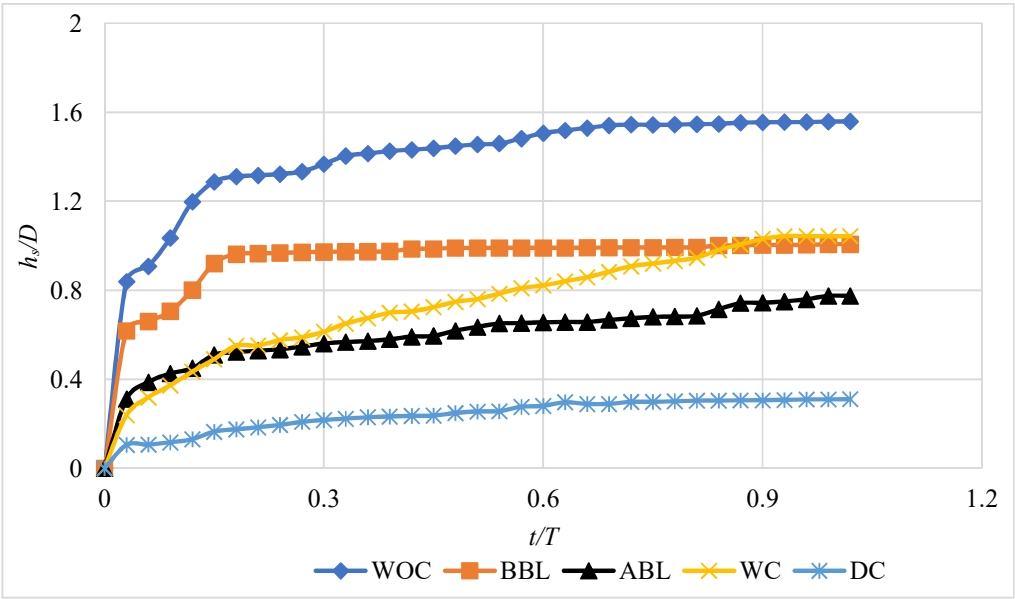


Figure 13: Temporal variation of scour depth ratio around Parabola faced pier for various conditions at 14 cm flow depth

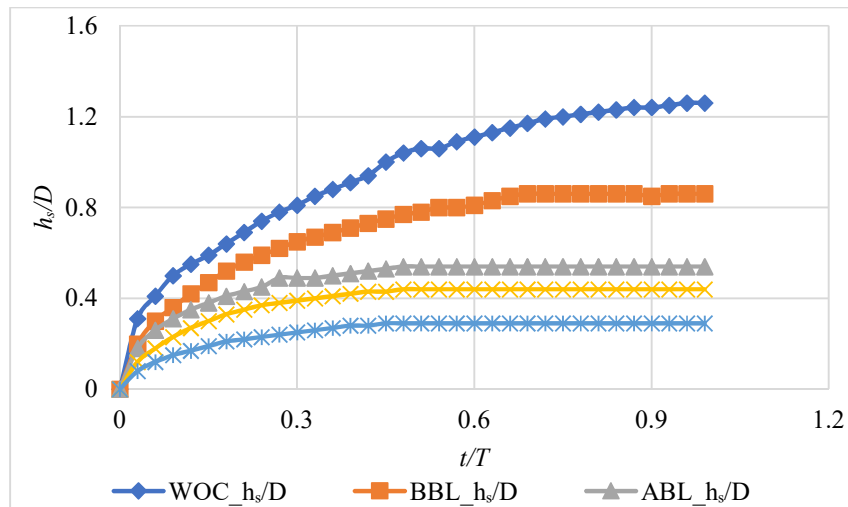


Figure 14: Temporal variation of scour depth ratio around Lenticular pier for various conditions at 12 cm flow depth

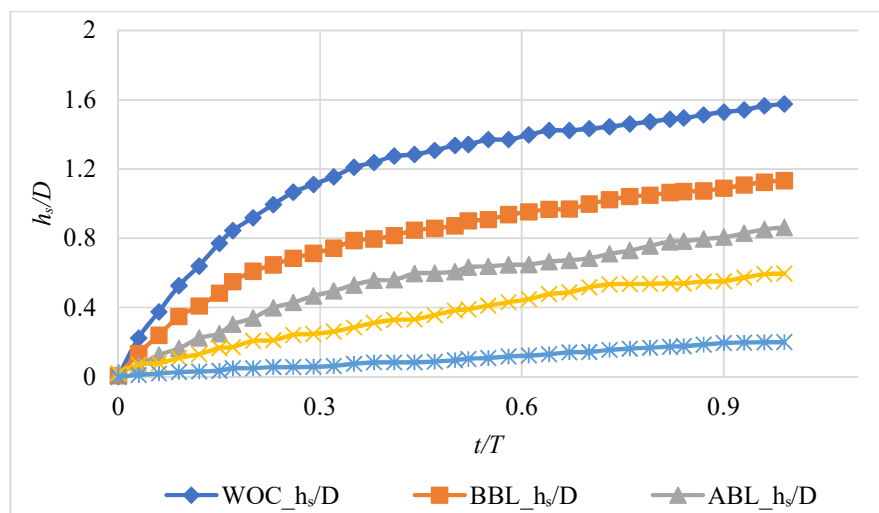


Figure 15: Temporal variation of scour depth ratio around Lenticular pier for various conditions at 14 cm flow depth

4.3 Effect of Collars on Modified Piers

Collar arrangements applied to modified pier shapes significantly improved scour reduction. The percentage reductions achieved with various collar placements were as follows:

a. Elliptical Pier:

- BL: 49.15% (Y = 12 cm), 43% (Y = 14 cm)
- 1DBBL: 23.88% (Y = 12 cm), 25% (Y = 14 cm)
- 1DABL: 17.91% (Y = 12 cm), 23.75% (Y = 14 cm)

- DC: 74.62% (Y = 12 cm), 66.25% (Y = 14 cm)

b. Parabolic Pier:

- BL: 54.54% (Y = 12 cm), 46.75% (Y = 14 cm)
- 1DBBL: 24.24% (Y = 12 cm), 27.27% (Y = 14 cm)
- 1DABL: 24.24% (Y = 12 cm), 25.97% (Y = 14 cm)
- DC: 77.27% (Y = 12 cm), 72.72% (Y = 14 cm)

c. Lenticular Pier:

- BL: 70.43% (Y = 12 cm), 56.49% (Y = 14 cm)
- 1DBBL: 20% (Y = 12 cm), 29.82% (Y = 14 cm)
- 1DABL: 58.62% (Y = 12 cm), 45.26% (Y = 14 cm)
- DC: 82.60% (Y = 12 cm), 77.54% (Y = 14 cm)

Collars placed at bed level and in DC configurations were the most effective. The results demonstrate the benefit of combining streamlined geometry with optimized collar placement.

4.4 Temporal Scour Development

In addition to analyzing maximum scour depths, it is critical to understand how quickly scour develops over time. This section examines the temporal evolution of scour across different pier shapes and collar configurations to assess their influence on the rate and stability of erosion under clear-water flow conditions.

Temporal variation of scour depth showed differences across pier shapes. Circular and elliptical piers developed scour more rapidly than parabolic and lenticular shapes. Lenticular piers delayed the onset of scour and reached equilibrium at shallower depths. Collar configurations also influenced the rate and extent of scour. Double collar (DC) setups consistently slowed scour progression and reduced final depths across all pier shapes. These trends are evident in previous discussions, where the scour depth over time clearly reflects the hydraulic influence of pier shape and collar configuration.

4.5 Scour Development in Two Piers in Tandem Arrangements

Following the analysis of temporal scour behavior in isolated pier models, the study progressed to evaluate the effects of multiple piers placed in tandem. These configurations are intended to simulate real-world scenarios where bridge piers are aligned along the direction of flow. The following section examines how the presence and shape of upstream piers influence the scour depth at downstream locations. The spacing between the piers was maintained as $S/D = 3$, where S is the center-to-center distance between piers and D is the pier diameter. A total of 22 experiments were performed, and the results are analyzed based on dimensionless scour depth (h_s/D) versus time (t/T). The findings illustrate variations in scour depth across different pier configurations and provide insights into the effectiveness of modified pier arrangements in reducing scour.

Experiments were conducted on two piers placed in tandem with identical spacing across all combinations. The results are illustrated using h_s/D vs. t/T graphs, where t/T is the ratio of actual

time to total experiment duration. A total of 10 different pier arrangements were examined, categorized into four combinations:

- Combination 1: CET, CPT, and CLT (Circular pier as the front pier)
- Combination 2: LCT, LET, and LPT (Lenticular pier as the front pier)
- Combination 3: ECT and ELT (Elliptical pier as the front pier)
- Combination 4: PCT and PLT (Parabolic pier as the front pier)

The maximum scour depth values around two piers in tandem for different configurations are detailed in Table 8.

Table 8: Maximum scour depth ratio (h_s/D) values around two piers in various tandem arrangements

Arrangement		<i>CET</i>	<i>CPT</i>	<i>CLT</i>	<i>LCT</i>	<i>LET</i>	<i>LPT</i>	<i>ECT</i>	<i>ELT</i>	<i>PCT</i>	<i>PLT</i>
h_s/D	Front pier	1.68	1.64	1.68	1.52	1.5	1.45	1.62	1.58	1.58	1.54
	Rear pier	1.28	1.04	0.80	1.38	1.45	1.12	1.3	0.78	1.34	0.80

(a) Combination 1 (Circular as Front Pier)

In Combination 1, where a circular pier was the front pier, the rear pier varied between elliptical, parabolic, and lenticular shapes. The scour depth around the isolated circular pier was observed to be $1.66D$, whereas in tandem arrangements, scour depth varied depending on the rear pier shape.

- In the CET arrangement, the scour depth around the rear elliptical pier was $1.28D$, representing a 20% reduction compared to an isolated elliptical pier.
- In the CPT arrangement, the scour depth around the rear parabolic pier was $1.04D$, yielding a 32.46% reduction compared to an isolated parabolic pier.
- In the CLT arrangement, the rear lenticular pier exhibited a scour depth of $0.80D$, marking a 43.85% reduction compared to an isolated lenticular pier.

The temporal variation of scour depth for these arrangements is illustrated in Figure 16.

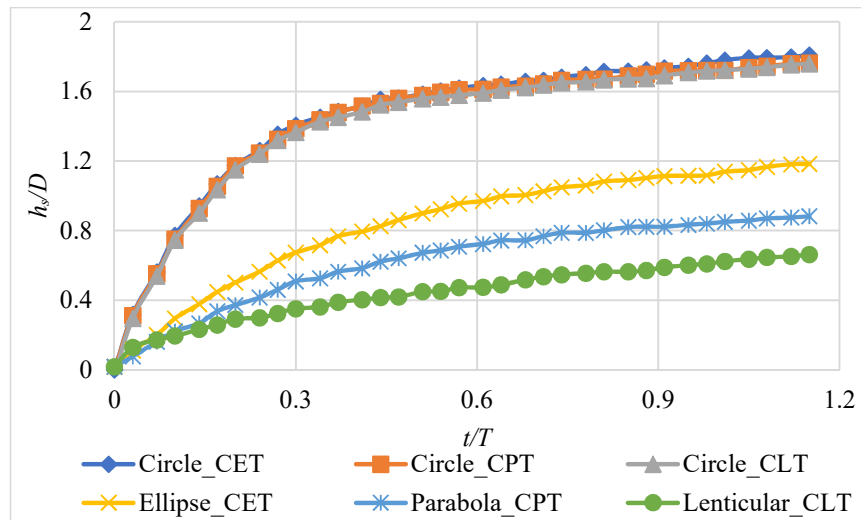


Figure 16: Temporal variation of scour depth ratio around two piers in tandem combination 1

(b) Combination 2 (Lenticular as Front Pier)

In Combination 2, the front pier was lenticular, while the rear pier was varied among circular, elliptical, and parabolic shapes.

- In the LCT arrangement, the rear circular pier exhibited a scour depth of 1.38D, 16.86% lower than an isolated circular pier.
- In the LET arrangement, the rear elliptical pier had a scour depth of 1.36D, reflecting a 15% reduction compared to an isolated elliptical pier.
- In the LPT arrangement, the rear parabolic pier had a scour depth of 1.12D, showing a 27.27% reduction compared to an isolated parabolic pier.

The temporal variation of scour depth for these arrangements is illustrated in Figure 17.

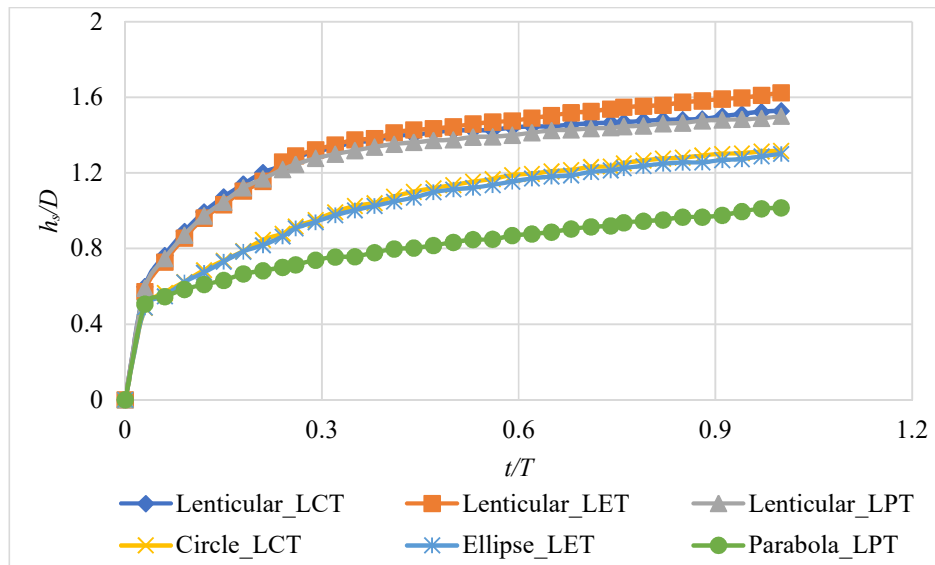


Figure 17: Temporal variation of scour depth ratio around two piers in tandem combination 2

(c) Combination 3 (Elliptical as Front Pier)

For Combination 3, where an elliptical pier was the front pier, the rear pier was circular or lenticular.

- In the ECT arrangement, the rear circular pier had a scour depth of 1.30D, showing 21.69% reduction compared to an isolated circular pier.
- In the ELT arrangement, the rear lenticular pier had a scour depth of 0.78D, marking a 45.26% reduction compared to an isolated lenticular pier.

The temporal variation of scour depth for these arrangements is illustrated in Figure 18.

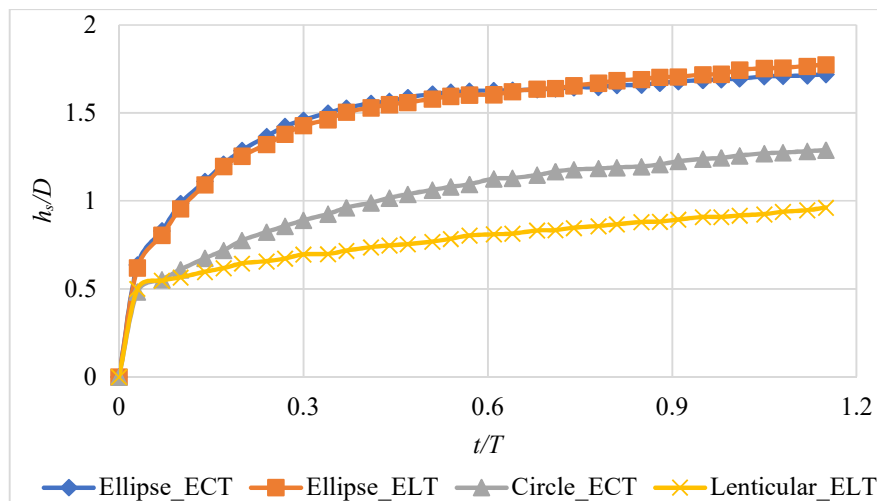


Figure 18: Temporal variation of scour depth ratio around two piers in tandem combination 3

(d) Combination 4 (Parabolic as Front Pier)

In Combination 4, where the front pier was parabolic, the rear pier was either circular or lenticular.

- In the PCT arrangement, the rear circular pier had a scour depth of 1.34D, indicating a 24.89% reduction compared to an isolated circular pier.
- In the PLT arrangement, the rear lenticular pier had a scour depth of 0.81D, showing a 43.22% reduction compared to an isolated lenticular pier.

The temporal variation of scour depth for these arrangements is illustrated in Figure 19.

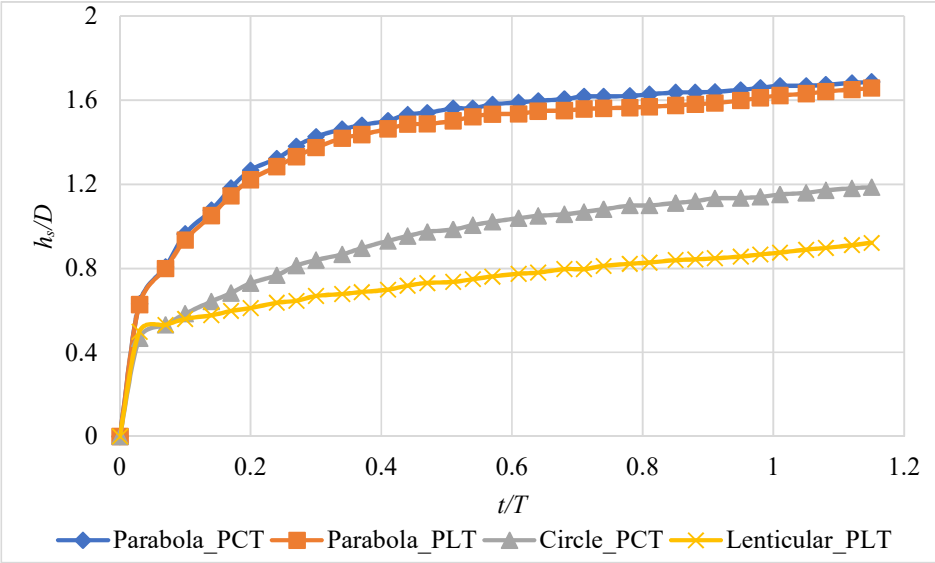


Figure 19: Temporal variation of scour depth ratio around 2 piers in tandem combination 4.

4.6 Scour Development in Three-Pier Tandem Arrangements

Experiments were conducted with three piers arranged in tandem, maintaining the same spacing between them ($S/D = 3$). A total of 12 different arrangements were examined, as listed in Table 9. The maximum scour depth values for three-pier configurations are provided in the table. The results highlight the influence of pier shape and positioning on scour depth variations. In all arrangements, the front pier experienced the highest scour due to direct flow exposure, while the rear pier benefited from a sheltering effect, leading to reduced scour. The variations in scour depth across different pier combinations are discussed below.

Table 9: Maximum scour depth ratio (h_s/D) values around three piers in various tandem arrangements

Arrangeme nt	<i>LCE</i> <i>T</i>	<i>LCP</i> <i>T</i>	<i>LCE</i> <i>T</i>	<i>LPC</i> <i>T</i>	<i>CEL</i> <i>T</i>	<i>CLP</i> <i>T</i>	<i>PCL</i> <i>T</i>	<i>PLC</i> <i>T</i>	<i>ELC</i> <i>T</i>	<i>ECL</i> <i>T</i>	<i>CLE</i> <i>T</i>	<i>CPL</i> <i>T</i>
-----------------	------------------------	------------------------	------------------------	------------------------	------------------------	------------------------	------------------------	------------------------	------------------------	------------------------	------------------------	------------------------

h_s/D	Front pier	1.42	1.54	1.54	1.47	1.68	1.66	1.52	1.56	1.62	1.6	1.66	1.64
	Middle pier	1.6	1.68	1.64	1.58	1.58	1.30	1.66	1.35	1.30	1.64	1.28	1.5
	Rear pier	1.28	1	1.3	1.38	0.85	1.02	0.83	1.36	1.32	0.80	1.32	0.78

The temporal variation of local scour in the LECT (Lenticular - Elliptical - Circular) arrangement is shown in Figure 20. In this arrangement, the middle elliptical pier experienced the highest scour depth (1.68D), influenced by secondary vortex formation. The front lenticular pier exhibited a moderate scour depth (1.54D), while the rear circular pier showed a 35.06% scour reduction compared to an isolated parabolic pier. This arrangement highlights the reinforcing effect on the middle pier, causing increased turbulence and scour, whereas the rear pier benefited from the flow shielding effect, leading to reduced scour.

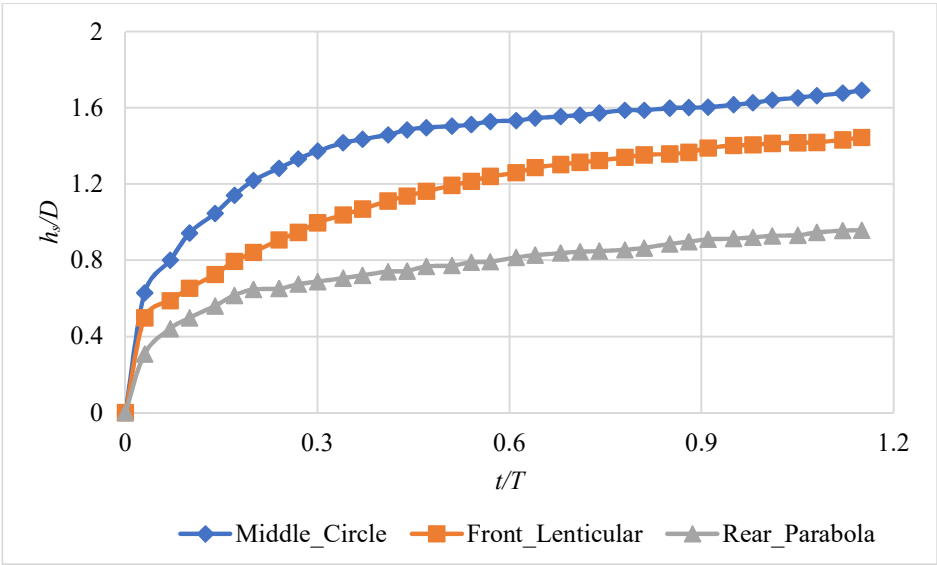


Figure 20: Temporal variation of local scour depth ratio around three piers in tandem in arrangement *LECT*

The temporal variation of local scour in the LCPT (Lenticular - Circular - Parabolic) arrangement is shown in Figure 21. In this arrangement, the middle circular pier had the highest scour depth (1.6D), as its blunt shape intensified turbulence and vortex strength. The front lenticular pier experienced moderate scour (1.425D), while the rear parabolic pier exhibited a 22.9% scour reduction compared to its isolated condition. The results suggest that the parabolic rear pier benefits from both the flow deflection from upstream piers and its streamlined shape in reducing scour depth.

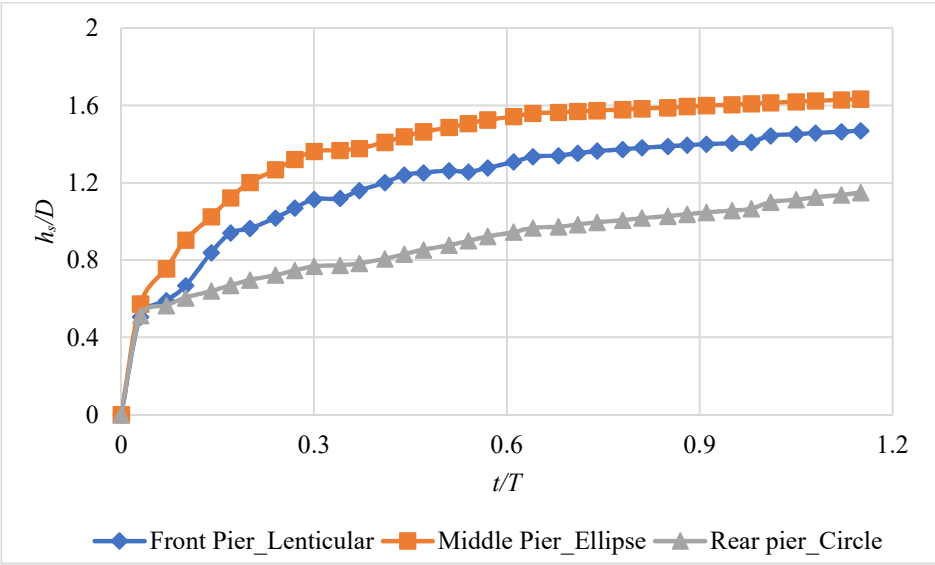


Figure 21: Temporal variation of local scour depth ratio around three piers in tandem in arrangement *LCPT*

The temporal variation of local scour in the LCET (Lenticular - Circular - Elliptical) arrangement is shown in Figure 22. In this arrangement, the circular middle pier exhibited the highest scour depth (1.64D) due to the stronger horseshoe vortex formation. The front lenticular pier had a scour depth of 1.54D, while the rear elliptical pier exhibited a gradual increase in scour over time, reaching 1.30D. The rear pier's scour reduction of 18.75% indicates that sheltering effects were weaker compared to other configurations, possibly due to its larger upstream face, which allowed sediment erosion to dominate over deposition effects.

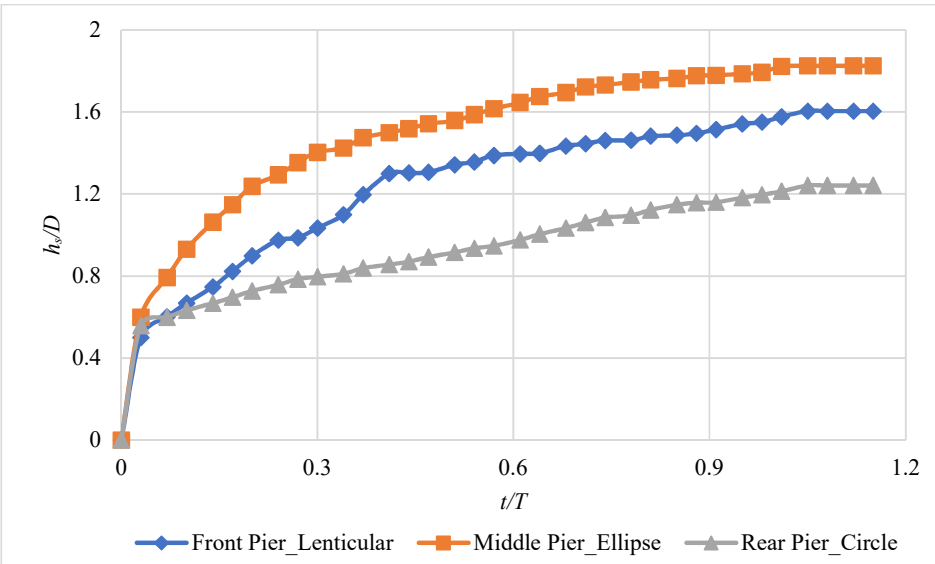


Figure 22: Temporal variation of local scour depth ratio around three piers in tandem in arrangement *LCET*

The temporal variation of local scour in the LPCT (Lenticular - Parabolic - Circular) arrangement is shown in Figure 23. In this arrangement, the middle parabolic pier exhibited the highest scour depth (1.58D), an unusual observation. The front lenticular pier, which typically shows reduced scour, had 1.47D scour depth, suggesting that the interaction of upstream flow did not significantly mitigate scour. The rear circular pier experienced a 16.75% scour reduction, which was lower than in other configurations, possibly due to weaker downflow effects caused by the combined influence of lenticular and parabolic piers.

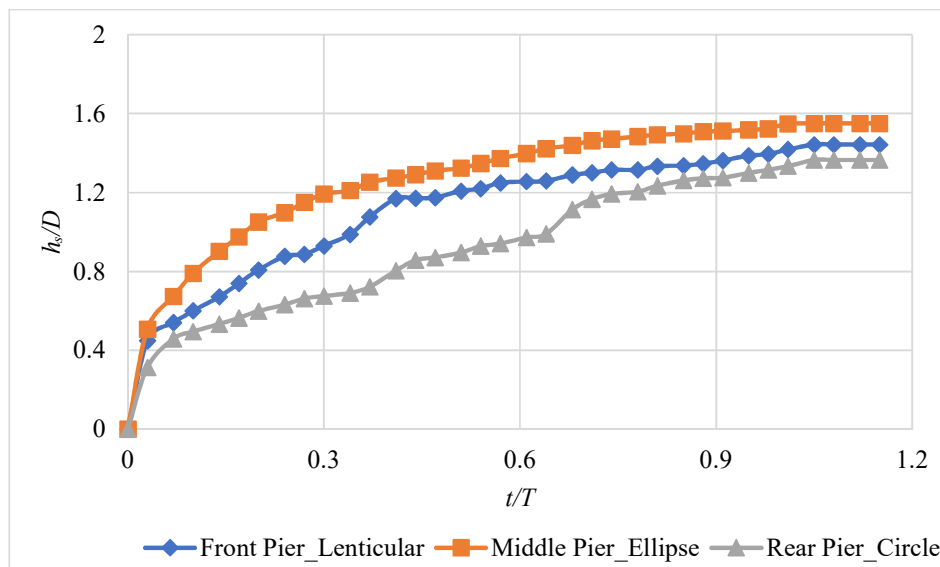


Figure 23: Temporal variation of local scour depth ratio around three piers in tandem in arrangement *LPCT*

The temporal variation of local scour in the CELT (Circular - Elliptical - Lenticular) arrangement is shown in Figure 24. This arrangement confirmed that a circular front pier produces the highest scour (1.68D) due to its large upstream face and reinforcing effect. The middle elliptical pier experienced moderate scour (1.58D), while the rear lenticular pier exhibited the lowest scour depth (0.85D), achieving a 40.35% reduction. This experiment demonstrated that placing a lenticular pier at the rear significantly minimizes scour due to its streamlined shape and the sheltering effect of the upstream piers.

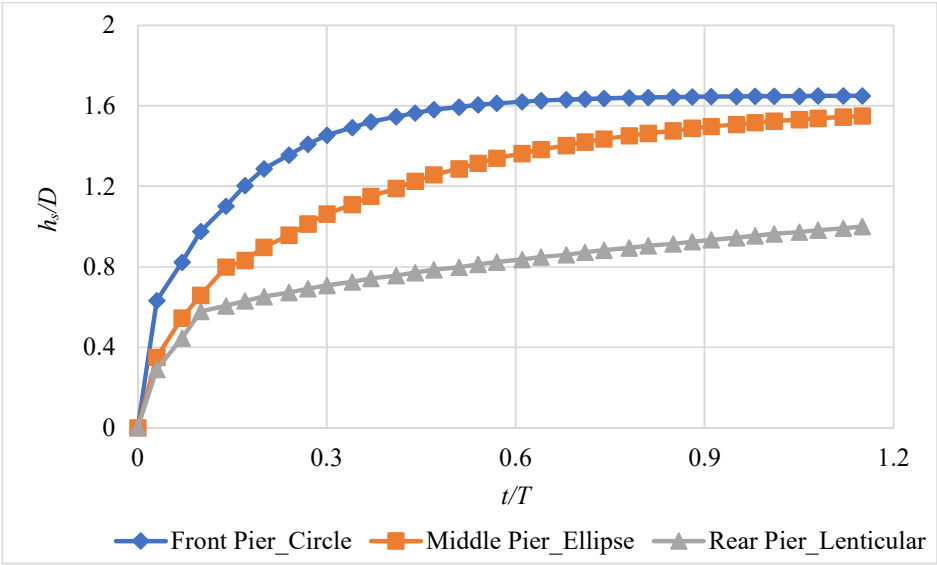


Figure 24: Temporal variation of local scour depth ratio around three piers in tandem in arrangement *CELT*

The temporal variation of local scour in the CLPT (Circular - Lenticular - Parabolic) arrangement is shown in Figure 25. In this arrangement, the front circular pier experienced the highest scour depth (1.66D), while the middle lenticular pier had a lower scour depth (1.30D) due to sediment deposition caused by vortices from the circular pier. The rear parabolic pier showed a 33.76% scour reduction, suggesting that sheltering effects were effective in mitigating scour at the rear position.

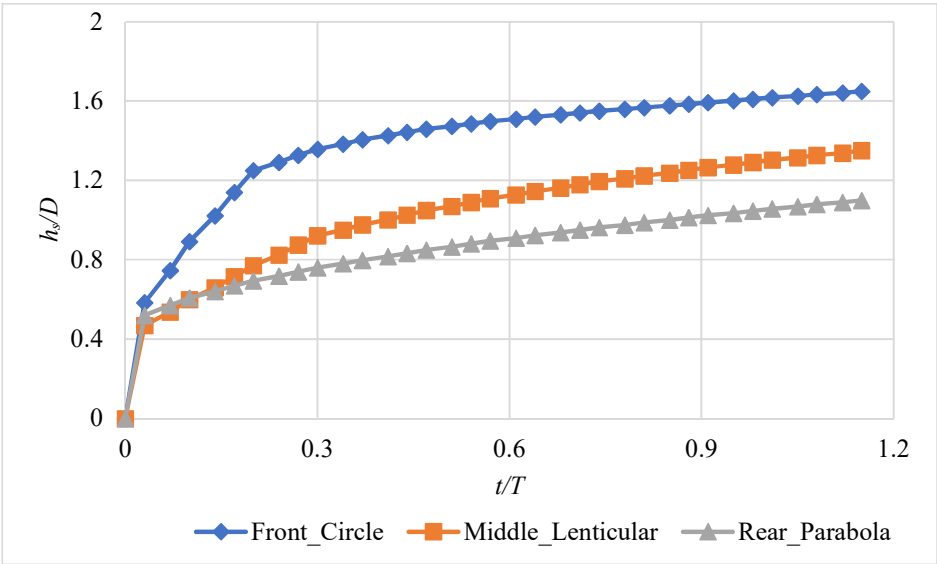


Figure 25: Temporal variation of local scour depth ratio around three piers in tandem in arrangement *CLPT*

The temporal variation of local scour in the PCLT (Parabolic - Circular - Lenticular) arrangement is shown in Figure 26. In this arrangement, the middle circular pier exhibited the highest scour depth (1.66D), while the rear lenticular pier had the lowest scour depth (0.83D), showing a 41.65% reduction. The scour reduction at the rear pier was due to sediment deposition at its upstream face, which delayed the scour progression and ultimately minimized sediment removal.

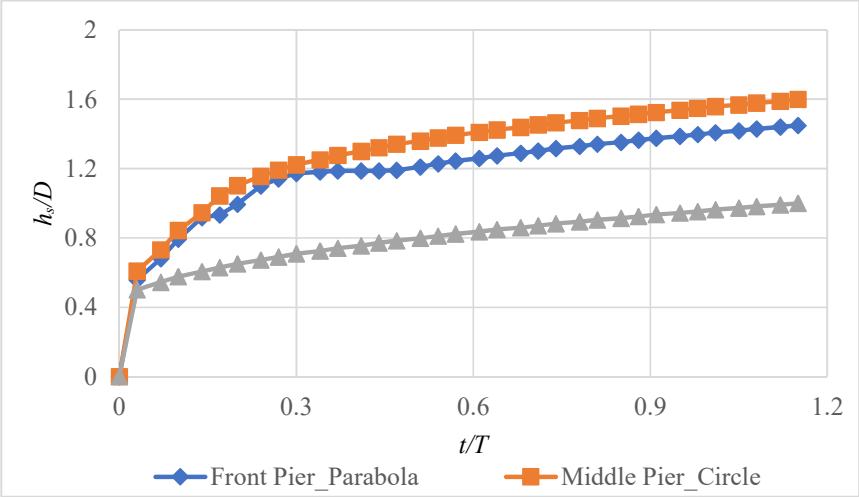


Figure 26: Temporal variation of local scour depth ratio around three piers in tandem in arrangement *PCLT*

The temporal variation of local scour in the PLCT (Parabolic - Lenticular - Circular) arrangement is shown in Figure 27. This arrangement showed that the front parabolic pier had the highest scour depth (1.56D), while the middle lenticular pier experienced a moderate scour depth of 1.35D. The rear circular pier, which typically experiences significant scour reduction, exhibited only an 18.07% reduction, suggesting that sheltering effects were less pronounced in this arrangement.

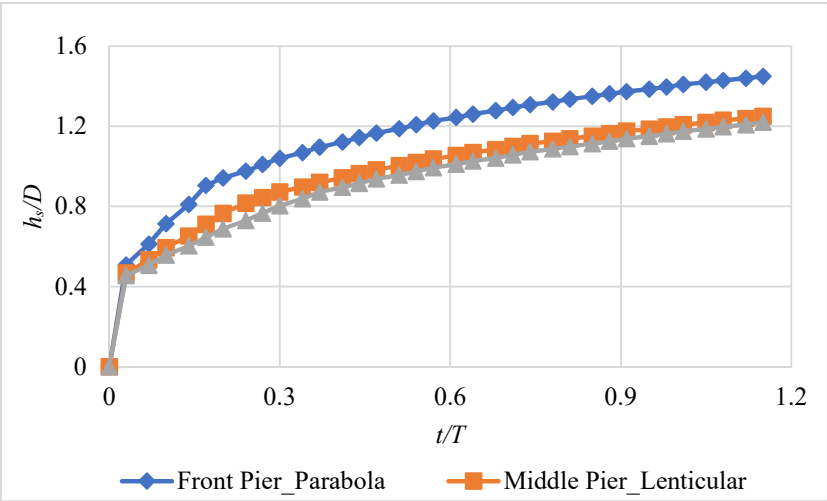


Figure 27: Temporal variation of local scour depth ratio around three piers in tandem in arrangement *PLCT*

The temporal variation of local scour in the ELCT (Elliptical - Lenticular - Circular) arrangement is shown in Figure 28. This arrangement demonstrated that the elliptical front pier had the highest scour depth (1.62D), while the middle lenticular pier had 1.30D scour depth, and the rear circular pier had 1.32D. The rear circular pier's scour reduction (20.48%) was lower than in other configurations, possibly due to the weaker sheltering effect of the lenticular middle pier.

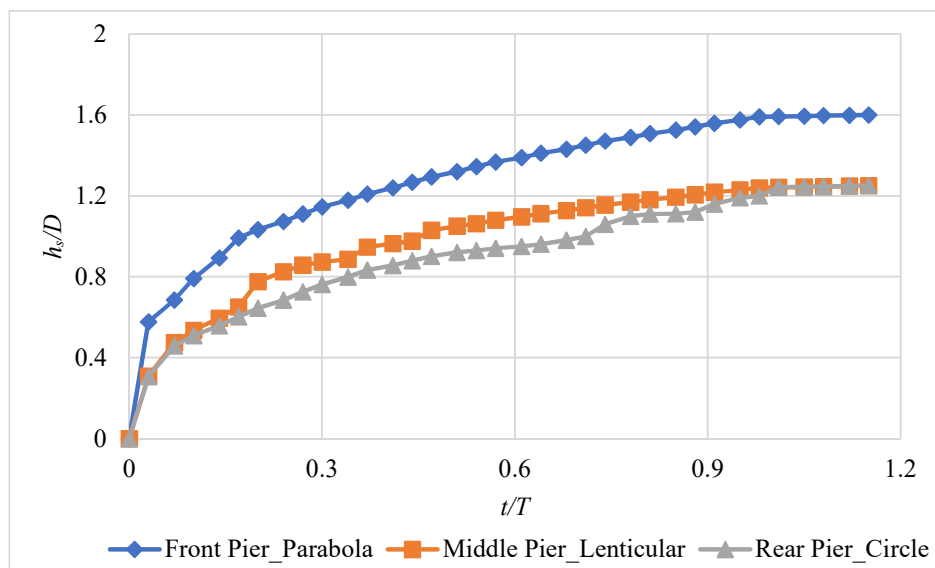


Figure 28: Temporal variation of local scour depth ratio around three piers in tandem in arrangement *ELCT*

The temporal variation of local scour in the ECLT (Elliptical - Circular - Lenticular) arrangement is shown in Figure 29. In this arrangement, the middle circular pier exhibited the highest scour depth (1.64D), while the rear lenticular pier had the lowest (0.80D), achieving a 43.22% reduction. The results indicate that placing a lenticular pier at the rear is an effective strategy for reducing scour.

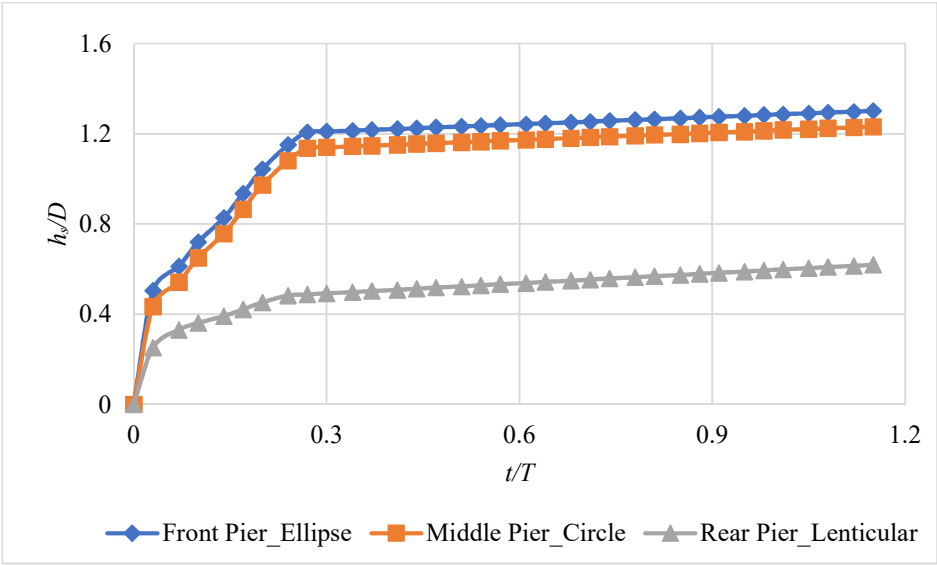


Figure 29: Temporal variation of local scour depth ratio around three piers in tandem in arrangement *ECLT*

The temporal variation of local scour in the CLET (Circular - Lenticular - Elliptical) arrangement is shown in Figure 30. This arrangement revealed that the front circular pier exhibited the highest scour depth (1.66D), while the middle lenticular pier had 1.28D, and the rear elliptical pier had 1.32D. The scour reduction at the rear elliptical pier (17.50%) was lower than in other setups, suggesting that the shape interaction between the lenticular and elliptical piers influenced the scour patterns differently compared to previous configurations.

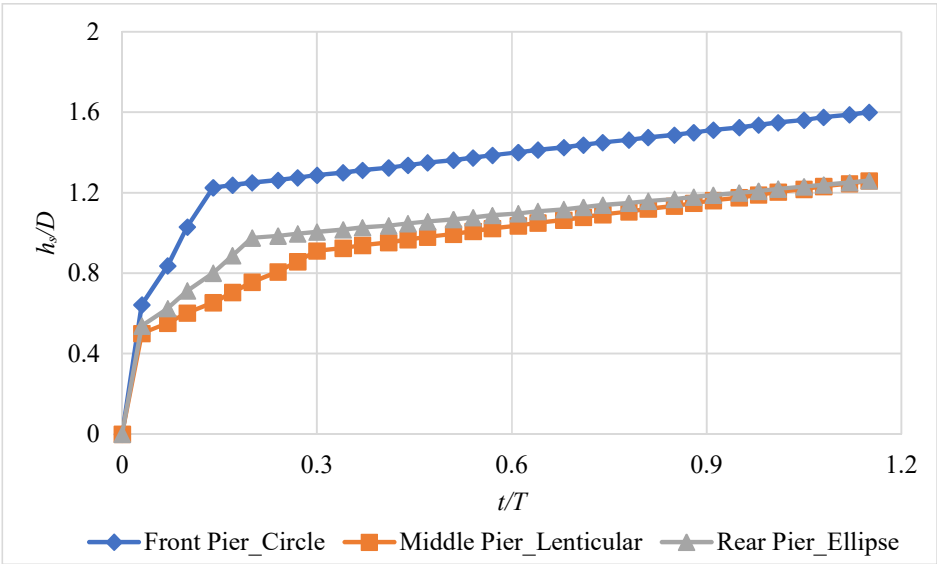


Figure 30: Temporal variation of local scour depth ratio around three piers in tandem in arrangement *CLET*

Finally, the CPLT arrangement (Circular - Parabolic - Lenticular), with temporal variation of local scour displayed in Figure 31, showed that the front circular pier exhibited high scour (1.64D), the middle parabolic pier experienced moderate scour (1.50D), and the rear lenticular pier had the lowest scour depth (0.78D), achieving a 44.91% reduction. This experiment confirms that placing a lenticular pier at the rear position in multi-pier arrangements is the most effective strategy for minimizing scour depth.

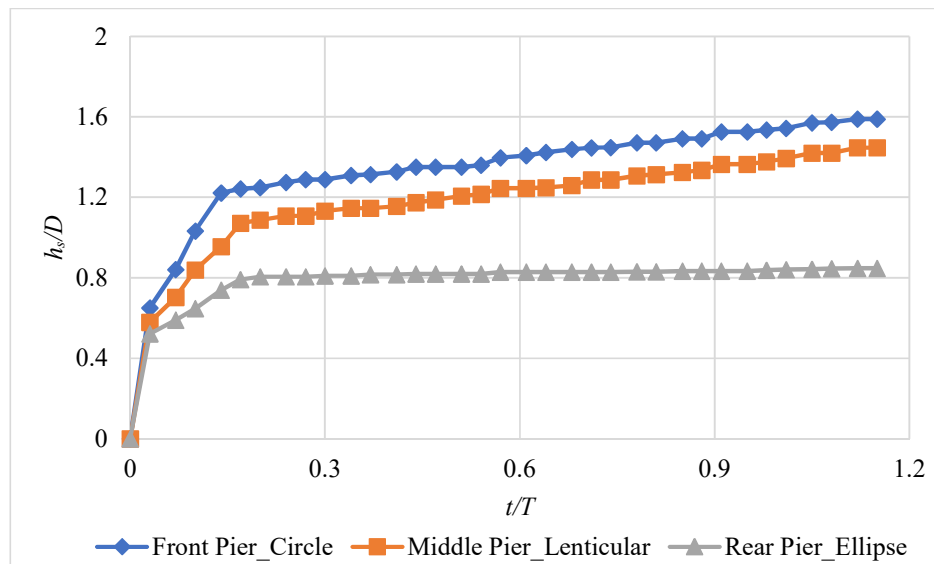


Figure 31: Temporal variation of local scour depth ratio around three piers in tandem in arrangement *CPLT*

Above results confirm that front piers experience the highest scour depth, while rear piers consistently show reduced scour due to the sheltering effect. Among the rear piers, lenticular piers consistently exhibited the lowest scour depths, demonstrating their effectiveness in multi-pier configurations. The scour reduction at rear piers ranged from 17.50% to 44.91%, with the highest reductions occurring in arrangements where the rear pier was lenticular. These findings reinforce the importance of pier shape and positioning in optimizing scour mitigation strategies for bridges with multiple piers.

4 Conclusions

This study systematically investigated the impact of modified pier shapes and collar placements on local scour around bridge piers under controlled laboratory conditions. Experiments were carried out using elliptical, parabolic, and lenticular piers, with a conventional circular pier serving as the baseline. Collar configurations tested included placement at bed level (BL), one diameter below bed level (1DBBL), one diameter above bed level (1DABL), and a double-collar setup (DC) to assess their effectiveness in mitigating scour. The study also extended to evaluate two-pier and three-pier tandem arrangements to examine scour interactions in multi-pier systems.

Among all configurations, the circular pier experienced the highest scour, with maximum scour depths reaching $1.38D$ ($Y = 12$ cm) and $1.66D$ ($Y = 14$ cm). Lenticular piers consistently delivered the greatest scour reduction, followed by parabolic and elliptical shapes. The inclusion of collars had a significant effect, particularly the double-collar arrangement, which achieved scour reductions of up to 72.46% and 65.06% for circular piers under 12 cm and 14 cm flow depths, respectively. Bed-level collars also performed well, while 1DBBL and 1DABL placements were comparatively less effective. When combined with modified shapes, the lenticular pier fitted with a double collar exhibited the minimum scour depth observed in the study.

In tandem arrangements, the front pier experienced elevated scour due to direct flow exposure, whereas the rear pier benefitted from sheltering. The greatest reduction, up to 45.26%, occurred when lenticular piers were placed at the rear. In three-pier configurations, the middle pier often exhibited the highest scour, especially when circular, due to intensified vortex interactions. Rear lenticular piers again demonstrated substantial reductions—up to 44.91%—confirming their optimal placement for minimizing scour in group pier systems. These findings reinforce the importance of both geometric modification and structural countermeasures in developing effective scour mitigation strategies. The lenticular pier, particularly in combination with a double-collar setup and rear positioning in tandem arrays, exhibited the most favorable performance. This study provides useful design insights for enhancing the resilience and stability of bridge foundations, particularly in scour-prone regions.

While the experimental results are promising, further research is essential to validate these findings at the field scale. Future work should focus on long-term monitoring of scour behavior around modified piers under natural flow conditions, numerical modeling to simulate and optimize flow-pier interactions, and the exploration of alternative collar materials and geometries. By advancing these research directions, a more comprehensive and resilient framework for bridge pier scour mitigation can be developed, contributing to safer and more sustainable transportation infrastructure.

References

1. Alireza, S., Mohammad, R., and Taghi, K. (2017). "Effect of Lenticular Piers on Scour Reduction." *Journal of Hydraulic Engineering*, 143(5), pp. 1–12.
2. Breusers, H.N.C., Nicollet, G., and Shen, H.W. (1977). "Local scour around cylindrical piers." *Journal of Hydraulic Research*, 15(3), pp. 211–252.
3. Chiew, Y.M. and Melville, B.W. (1987). "Local scour around bridge piers." *Journal of Hydraulic Research*, 25(1), pp. 15–26.
4. Grimaldi, C., Gaudio, R., and Calomino, F. (2009). "Experimental study on scour at bridge piers." *Journal of Hydraulic Engineering*, 135(2), pp. 117–124.
5. Heidarpour, M., Afzalimehr, H., and Omid, M.H. (2010). "Reduction of local scour in the vicinity of bridge pier groups using collars and slots." *Journal of Hydraulic Research*, 48(5), pp. 656–661.
6. IRC (Indian Roads Congress). (2000). *Guidelines for the Design of Bridge Foundations*. IRC:78-2000, Indian Roads Congress, New Delhi.

7. Kothiyari, U.C. (2007). "Scour around bridge piers and abutments." *Journal of Hydraulic Engineering*, 133(3), pp. 291–297.
8. Lacey, G. (2003). "Scour at bridge piers: Empirical approaches." *Journal of Hydraulic Engineering*, 129(2), pp. 120–129.
9. Laursen, E. M., and Toch, A. (1956). *Scour around bridge piers and abutments*. Bulletin No. 4, Iowa Highway Research Board, Ames, Iowa.
10. Mashahir, A., Ghodsian, M., and Vaghefi, M. (2006). "Local scour reduction around bridge piers using submerged vanes." *Journal of Hydraulic Engineering*, 132(3), pp. 236–241.
11. Melville, B.W. and Coleman, S.E. (2000). *Bridge scour*. Water Resources Publications, LLC.
12. Melville, B.W. and Hadfield, A.C. (1999). "Countermeasures against scour at bridge piers." *Journal of Hydraulic Engineering*, 125(5), pp. 455–464.
13. Mia, M.B. and Nago, H. (2003). "Design method of time-dependent local scour at bridge piers." *Journal of Hydraulic Engineering*, 129(6), pp. 420–426.
14. Mohammad, R., Alireza, S., and Taghi, K. (2010) "Experimental study on the influence of collar position on scour depth around bridge piers." *Journal of Hydraulic Research*, 48(1), pp. 135–143.
15. Moncada, M., Cardoso, A.H., and Borges, J.L. (2009). "Scour around bridge piers with collars: Laboratory study." *Journal of Hydraulic Engineering*, 135(7), pp. 587–592.
16. Mubeen Beg, M., Ahmad, Z., and Aziz, N.M. (2013). "Experimental study on flow characteristics around bridge piers of different shapes." *Journal of Hydraulic Research*, 51(5), pp. 595–607.
17. Shen, H.W., Schneider, V.R., and Karaki, S. (1969). "Local scour around bridge piers." *Journal of the Hydraulics Division*, 95(6), pp. 1919–1940.
18. Tseng, W.S., Hsu, S.M., and Yang, J.C. (2000). "Scour protection around bridge piers using collar structures." *Journal of Hydraulic Engineering*, 126(6), pp. 475–483.
19. Zarrati, A.R., Nazariha, M., and Mashahir, A. (2004) "Reduction of local scour in the vicinity of bridge pier groups using collars." *Journal of Hydraulic Research*, 42(2), pp. 161–167.
20. B. Kumar, V. Singh Study of scour near pier of Gandhi setu in Ganga River Water Sci. Technol. Libr., 110 (2022)
21. H. Omara, O.K. Saleh, M. Al-Mutiry, A. Masria, A. Tawfik Assessment the local scour around vertical and inclined oblong piers under shallow flow condition Ocean Eng., 281 (15) (2023), pp. 1-13
22. S. Dey, S.K. Zeeshan Ali The universal two-fifths law of pier scour Phys. Fluids, 36 (2024)
23. A. Bagheri, A. Bordbar, M. Heidarnajad, A. Masjedi In-depth simulation of netted collars on scour depth control using machine-learning models Results in Engineering, 21 (2024), Article 101820.
24. D. Dutta, M. Saud Afzal Scour around twin-piles under combined wave-current flows Coastal Engineering, 189 (2024), Article 104477.
25. A. Baranwal, B.S. Das "Scouring around bridge pier: a comprehensive analysis of scour depth predictive equations and live bed scouring conditions AQUA- Water Infrastructure, Ecosystem and society, 73 (3) (2024), pp. 424-452